

Article

Crossover Induced Electron Pairing and Superconductivity by Kinetic Renormalization in Correlated Electron Systems

Takashi Yanagisawa ^{1,*}, Mitake Miyazaki ² and Kunihiko Yamaji ¹

¹ National Institute of Advanced Industrial Science and Technology 1-1-1 Umezono, Tsukuba, Ibaraki 305-8568, Japan; yamaji@xf7.so-net.ne.jp

² Hakodate Institute of Technology, 14-1 Tokura, Hakodate, Hokkaido 042-8501, Japan; miyazaki@hakodate-ct.ac.jp

* Correspondence: t-yanagisawa@aist.go.jp

Received: 30 June 2018; Accepted: 5 September 2018; Published: 6 September 2018



Abstract: We investigate the ground state of strongly correlated electron systems based on an optimization variational Monte Carlo method to clarify the mechanism of high-temperature superconductivity. The wave function is optimized by introducing variational parameters in an exponential-type wave function beyond the Gutzwiller function. The many-body effect plays an important role as an origin of superconductivity in a correlated electron system. There is a crossover between weakly correlated region and strongly correlated region, where two regions are characterized by the strength of the on-site Coulomb interaction U . We insist that high-temperature superconductivity occurs in the strongly correlated region.

Keywords: strongly correlated electron systems; mechanism of superconductivity; high-temperature superconductivity; kinetic mechanism of superconductivity; optimization variational Monte Carlo method; Hubbard model

1. Introduction

The mechanism of high-temperature superconductivity has been studied vigorously for more than 30 years since the discovery of cuprate high-temperature superconductors [1]. High-temperature cuprates are typical strongly correlated systems since the parent materials are Mott insulators when no carriers are doped. It is important to understand electronic properties of strongly correlated electron systems.

The CuO_2 plane is commonly contained in high-temperature cuprates, where the CuO_2 plane consists of oxygen atoms and copper atoms. The electronic model for this plane is called the d-p model (or three-band Hubbard model) [2–18]. It appears very hard to elucidate the phase diagram of the d-p model because of strong correlation between electrons. We often examine simplified models such as the two-dimensional single-band Hubbard model [19–38] or ladder model [39–43] as an attempt to make clear the phase diagram of correlated electron systems.

The Hubbard model is one of the fundamental models in the study of condensed matter physics. The Hubbard model is employed to understand the metal-insulator transition [44] and magnetic properties of various compounds [45,46]. The Hubbard model and also the d-p model have the potential to explain various phenomena. By employing the Hubbard model, we can understand the appearance of inhomogeneous states, reported for cuprates, such as stripes [47–54] and checkerboard-like density wave states [55–58].

It is important to clarify whether high-temperature superconductivity can be explained based on the Hubbard model (and the three-band d-p model). Previous works on the ladder Hubbard model supported the existence of superconducting phase [39–43,59]. Recent studies on the two-dimensional

(2D) Hubbard model show positive results on superconductivity (SC) [38]. We show the order parameters of antiferromagnetic (AF) state and SC state as a function of the interaction parameter U in Figure 1. We think that the result strongly supports the existence of SC and shows a possibility of high-temperature superconductivity in the strongly correlated region.

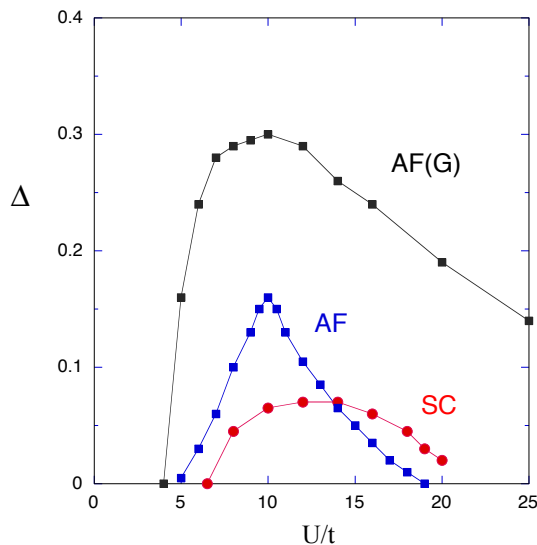


Figure 1. AF and SC order parameters as a function of U/t on a 10×10 lattice with the periodic boundary condition in one direction and antiperiodic one in the other direction [38]. In Reference [38] Δ was shown as a function of U in the range $0 < U < 20$. We modified the figure to include the range $20 < U < 25$. Δ_{AF} has a peak when U is of the order of the bandwidth $U/t \sim 10$. AF(G) in the figure shows the result obtained for the simple Gutzwiller function.

A variational Monte Carlo method is a useful method to investigate electronic properties of strongly correlated electron systems by calculating the expectation values numerically [26–31]. A variational wave function can be improved by introducing new variational parameters to control the electron correlation. We have proposed wave functions that are optimized by multiplying an initial function by $\exp(-S)$ -type operators [38,60,61], where S is a suitable correlation operator. The Gutzwiller function is also written in this form. An optimization process is performed in a systematic way by multiplying by the exponential-type operators repeatedly [60]. The ground-state energy is lowered considerably by using this type of wave functions [38]. This paper can be viewed as an extension of the paper published in proceeding of conference on superconductivity (ISS2017) [62].

2. Model Hamiltonians

The Hubbard model is written as

$$H = \sum_{ij\sigma} t_{ij} c_{i\sigma}^\dagger c_{j\sigma} + U \sum_i n_{i\uparrow} n_{i\downarrow}, \tag{1}$$

where t_{ij} indicates the transfer integral and U is the strength of the on-site Coulomb interaction. We set $t_{ij} = -t$ when i and j are nearest-neighbor pairs $\langle ij \rangle$ and $t_{ij} = -t'$ when i and j are next-nearest neighbor pairs. We consider this model in two dimensions, and N and N_e denote the number of lattice sites and the number of electrons, respectively.

We also consider the three-band model that explicitly contains oxygen p and copper d electrons. The Hamiltonian is

$$\begin{aligned}
 H_{dp} = & \epsilon_d \sum_{i\sigma} d_{i\sigma}^\dagger d_{i\sigma} + \epsilon_p \sum_{i\sigma} (p_{i+\hat{x}/2\sigma}^\dagger p_{i+\hat{x}/2\sigma} + p_{i+\hat{y}/2\sigma}^\dagger p_{i+\hat{y}/2\sigma}) \\
 & + t_{dp} \sum_{i\sigma} [d_{i\sigma}^\dagger (p_{i+\hat{x}/2\sigma} + p_{i+\hat{y}/2\sigma} - p_{i-\hat{x}/2\sigma} - p_{i-\hat{y}/2\sigma}) + \text{h.c.}] \\
 & + t_{pp} \sum_{i\sigma} [p_{i+\hat{y}/2\sigma}^\dagger p_{i+\hat{x}/2\sigma} - p_{i+\hat{y}/2\sigma}^\dagger p_{i-\hat{x}/2\sigma} \\
 & - p_{i-\hat{y}/2\sigma}^\dagger p_{i+\hat{x}/2\sigma} + p_{i-\hat{y}/2\sigma}^\dagger p_{i-\hat{x}/2\sigma} + \text{h.c.}] \\
 & + t'_d \sum_{\langle\langle ij \rangle\rangle\sigma} \epsilon_{ij} (d_{i\sigma}^\dagger d_{j\sigma} + \text{h.c.}) + U_d \sum_i d_{i\uparrow}^\dagger d_{i\uparrow} d_{i\downarrow}^\dagger d_{i\downarrow} \\
 & + U_p \sum_i (n_{i+\hat{x}/2\uparrow}^p n_{i+\hat{x}/2\downarrow}^p + n_{i+\hat{y}/2\uparrow}^p n_{i+\hat{y}/2\downarrow}^p). \tag{2}
 \end{aligned}$$

We use the hole picture in this paper. $d_{i\sigma}$ and $d_{i\sigma}^\dagger$ represent the operators for the d hole. $p_{i\pm\hat{x}/2\sigma}$ and $p_{i\pm\hat{y}/2\sigma}^\dagger$ denote the operators for the p holes at the site $R_{i\pm\hat{x}/2}$, and in a similar way $p_{i\pm\hat{y}/2\sigma}$ and $p_{i\pm\hat{x}/2\sigma}^\dagger$ are defined. $n_{i+\hat{x}/2\sigma}^p$ and $n_{i+\hat{y}/2\sigma}^p$ denote the number operators of p holes at $R_{i+\hat{x}/2}$ and $R_{i+\hat{y}/2}$, respectively. t_{dp} is the transfer integral between adjacent Cu and O orbitals and t_{pp} is that between nearest p orbitals. t'_d indicates that between d orbitals where $\langle\langle ij \rangle\rangle$ denotes a next nearest-neighbor pair of copper sites. cuprate superconductors such as $\text{Bi}_2\text{Sr}_2\text{CaCu}_2\text{O}_{8+\delta}$ [63] and $\text{Tl}_2\text{Ba}_2\text{CuO}_{6+\delta}$ [64]. ϵ_{ij} takes the values ± 1 according to the sign of the transfer integral between next nearest-neighbor d orbitals. U_d is the strength of the on-site Coulomb repulsion between d holes and U_p is that between p holes. We can reproduce the Fermi surface by using parameters t_{dp} , t_{pp} and t'_d . The values of band parameters have been estimated [65–69]; for example, $U_d = 10.5$, $U_p = 4.0$ and $U_{dp} = 1.2$ in eV [66] where U_{dp} is the nearest-neighbor Coulomb interaction between holes on adjacent Cu and O orbitals. We neglect U_{dp} because U_{dp} is small compared to U_d . We use the notation $\Delta_{dp} = \epsilon_p - \epsilon_d$. The number of sites is denoted as N , and the total number of atoms is $N_a = 3N$. The energy unit is given by t_{dp} .

3. Optimization Variational Monte Carlo Method

In a variational Monte Carlo method, we employ a wave function that is suitable for the system which we consider and evaluate the expectation values by using a Monte Carlo procedure. To take into account electron correlation between electrons, we start from the Gutzwiller wave function given by

$$\psi_G = P_G \psi_0, \tag{3}$$

where P_G is the Gutzwiller operator $P_G = \prod_j (1 - (1 - g)n_{j\uparrow}n_{j\downarrow})$ where g is the variational parameter in the range of $0 \leq g \leq 1$. ψ_0 indicates a trial one-particle state.

Because the Gutzwiller function is very simple and is not enough to take account of electron correlation, we should improve the wave function. There are several methods to optimize the wave function. One method is to multiply the Gutzwiller function by an exponential-type operator. The wave function is written as [38,60,70–74]

$$\psi_\lambda = \exp(-\lambda K) \psi_G, \tag{4}$$

where K is the kinetic part of the Hamiltonian and λ is a real variational operator [31,60,71]. The expectation values are calculated by using the auxiliary field method [60,75]. The other method to improve the Gutzwiller function is to introduce a Jastrow-type operator [33]. We can control nearest-neighbor correlation by multiplying by the operator

$$P_{Jdh} = \prod_j \left(1 - (1 - \eta) \prod_\tau \left[d_j (1 - e_{j+\tau}) + e_j (1 - d_{j+\tau}) \right] \right), \tag{5}$$

where d_j is the operator for the doubly-occupied site given as $d_j = n_{j\uparrow}n_{j\downarrow}$ and e_j is that for the empty site given by $e_j = (1 - n_{j\uparrow})(1 - n_{j\downarrow})$. η is the variational parameter in the range $0 \leq \eta \leq 1$. With this operator we can include the doublon-holon correlation:

$$\psi_\eta = P_{Jdh}\psi_G. \quad (6)$$

It is possible to generalize the Jastrow operator to consider long-range electron correlation by introducing new variational parameters [76].

In this paper we use the wave function of exponential type in Equation (4). We call this type of wave function the off-diagonal wave function since the off-diagonal correlation in the site representation is taken into account in this wave function. We believe that it is more important to consider off-diagonal electron correlation than diagonal electron correlation. In fact, the energy is further lowered when we employ the off-diagonal wave function [38].

4. Antiferromagnetic Crossover

The AF one-particle state ψ_{AF} is given by the eigenfunction of the AF trial Hamiltonian given by

$$H_{AF} = \sum_{ij\sigma} t_{ij} c_{i\sigma}^\dagger c_{j\sigma} - \Delta_{AF} \sum_{i\sigma} (-1)^{x_i+y_i} \sigma n_{i\sigma}, \quad (7)$$

where Δ_{AF} is the AF order parameter and (x_i, y_i) represents the coordinates of the site i . With ψ_{AF} , the wave function is given as

$$\psi_{\lambda,AF} = \exp(-\lambda K) P_G \psi_{AF}. \quad (8)$$

In general, the AF state is very stable in the Hubbard model near half-filling. Thus, it is important to control AF magnetic order so that the superconducting state is realized. The 2D Hubbard model and the three-band d-p model have similarity with respect to magnetic order. We found that the AF state is more stable in the d-p model than in the single-band Hubbard model.

The stability of the AF state depends mainly on the electron density n_e , the interaction strength U , and the transfer integral t' and long-range transfers in the single-band Hubbard model. The AF correlation is induced as U increases from zero in weakly correlated region and is maximized when U is of the order of the bandwidth, say at $U = U_c$, when carriers are doped. When U becomes larger than U_c , the AF correlation turns to decrease. In the region where U is extremely large, the AF correlation is suppressed to a small value by large fluctuation. This is shown in Figure 1. Thus, there is a crossover between weakly correlated region and strongly correlated region.

The transfer integral t' also shows non-trivial effect on the stability of AF magnetic order. As $-t'$ increases, the AF correlation increases. (We adopt that t' is negative in this paper.) We show Δ_{AF} as a function of $1 - n_e$ in Figure 2 for $t' = 0$ and Figure 3 for $t' = -0.2$. When t' is negative, the AF region expands up to about 20 percent doping where $1 - n_e \sim 0.2$.

In the three-band d-p model, the AF correlation is stronger than that in the single-band Hubbard model. We introduced the transfer integral t'_d to control the strength of antiferromagnetism. We found that the AF correlation is reduced when t'_d increases, which is in contrast to the role of t' for the Hubbard model. The Figure 4 shows the phase diagram of the ground state in the half-filled case in the $t_{pp} - t'_d$ plane where AFI and PI indicate antiferromagnetic insulator state and paramagnetic insulator state, respectively. A phase transition occurs from the antiferromagnetic insulator to the paramagnetic insulator as parameters t_{pp} and t'_d increase. A copper oxide which is an insulator without hole doping may be in the AFI region of this figure. For such copper oxides, $|t'_d|$ may not be very large and we expect that the value of t'_d may be in the range $|t'_d| \leq -0.2t_d$. As the density of holes increases, the role of t'_d and t_{pp} will become important.

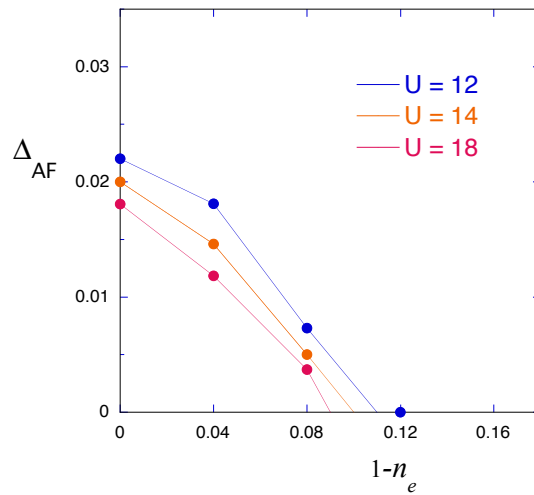


Figure 2. Antiferromagnetic order parameters as a function of the hole density $1 - n_e$ on a 10×10 lattice for $t' = 0$. We put $U/t = 12, 14$ and 18 .

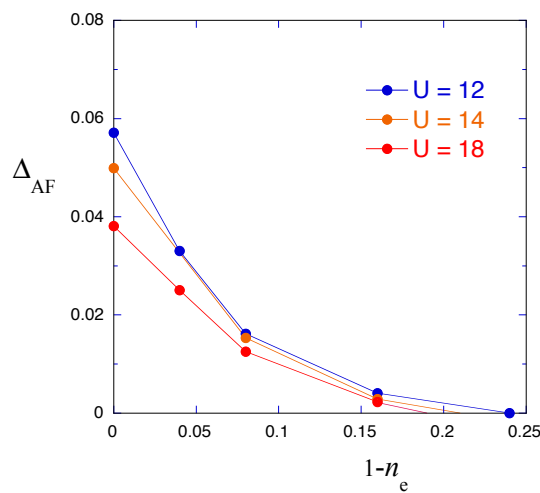


Figure 3. Antiferromagnetic order parameters as a function of the hole density $1 - n_e$ on a 10×10 lattice for $t' = -0.2t$. We put $U/t = 12, 14$ and 18 .

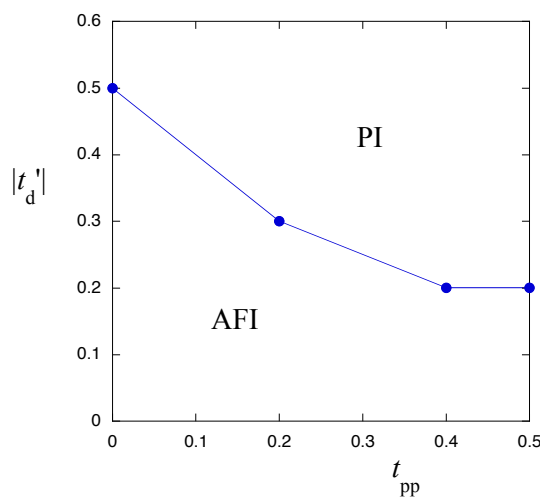


Figure 4. Antiferromagnetic and paramagnetic insulator states in the plane of t_{pp} and $|t'_d|$ for the d-p model. We put $U_d = 8, U_p = 0, \epsilon_p - \epsilon_d = 1$ and $t'_d < 0$ on a 6×6 lattice with 108 atoms in total. The energy unit is given by t_{dp} .

5. Correlated Superconductivity

The superconducting state is represented by the BCS wave function

$$\psi_{BCS} = \prod_k (u_k + v_k c_{k\uparrow}^\dagger c_{-k\downarrow}^\dagger) |0\rangle, \tag{9}$$

with coefficients u_k and v_k that appear in the ratio $u_k/v_k = \Delta_k / (\zeta_k + \sqrt{\zeta_k^2 + \Delta_k^2})$, where Δ_k is the gap function with \mathbf{k} dependence and $\zeta_k = \epsilon_k - \mu$ is the dispersion relation of conduction electrons. We assume the d -wave symmetry for Δ_k : $\Delta_k = \Delta_{SC}(\cos k_x - \cos k_y)$. The Gutzwiller BCS state is formulated as

$$\psi_{G-BCS} = P_{N_e} P_G \psi_{BCS}, \tag{10}$$

where P_{N_e} indicates the operator to extract the state with N_e electrons. In this wave function the electron number is fixed and thus the chemical potential in ζ_k is regarded as a variational parameter. In the formulation of ψ_λ , we use the BCS wave function without fixing the total electron number, namely, without the operator P_{N_e} . The chemical potential μ in ζ_k is not a variational parameter and is used to adjust the total electron number. The wave function is given as

$$\psi_\lambda = e^{-\lambda K} P_G \psi_{BCS}. \tag{11}$$

We perform the electron-hole transformation for down-spin electrons:

$$d_k = c_{-k\downarrow}^\dagger, \quad d_k^\dagger = c_{-k\downarrow}, \tag{12}$$

and not for up-spin electrons: $c_k = c_{k\uparrow}$. The electron pair operator $c_{k\uparrow}^\dagger c_{-k\downarrow}^\dagger$ denotes the hybridization operator $c_k^\dagger d_k$ in this formulation.

We show the phase diagram in Figure 5 where the condensation energies for SC and AF states are shown as a function of the hole density $1 - n_e$ for $U/t = 18$ and $t' = 0$. The condensation energy ΔE is defined as the energy lowering due to the inclusion of the order parameter:

$$\Delta E = E(\Delta = 0) - E(\Delta_{opt}), \tag{13}$$

where Δ is the SC or AF order parameter and Δ_{opt} is its optimized value. We set $t' = 0$ because $t' = 0$ is the most optimal parameter value for superconductivity. In the optimum range for superconductivity, a pure d -wave superconducting state is realized.

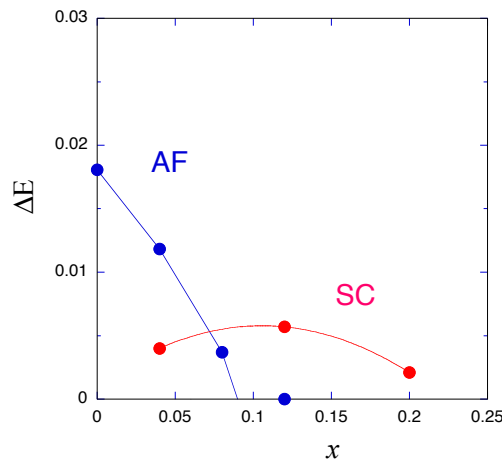


Figure 5. The condensation energy per site as a function of the hole density $x = 1 - n_e$ on a 10×10 lattice for the 2D Hubbard model. The SC and AF condensation energies are shown. We set $t' = 0$ and $U/t = 18$.

As shown in Figure 5, there is a coexistence of superconductivity and antiferromagnetism when the doping rate $x < 0.09$. There is a possibility of coexistence in the underdoped region. This may be related to unusual metallic properties of cuprate superconductors in the underdoped region. We expect that the area of coexistence phase becomes smaller as the wave function is improved and optimized further by multiplying by exponential correlation operators.

6. Phase Separation

We discuss the phase separation in the 2D Hubbard model here. An existence of the phase separation has been pointed out recently. The ground-state energy $E(N_e)$, where N_e is the number of electrons, may exhibit a singular behavior near half-filling when the ground-state energy at half-filling is lowered extremely due to the AF order. The quantity $\delta^2 E(N_e) \equiv [E(N_e + \delta N_e) - 2E(N_e) + E(N_e - \delta N_e)]/(\delta N_e)^2$, being proportional to the second derivative of the energy $E(N_e)$ with respect to the electron number, has a possibility to be negative for low hole doping. The phase separation occurs when $\delta^2 E(N_e)$ is negative. In our optimized wave function, the phase separation is restricted to the range $x \equiv 1 - n_e \leq 0.06$ for $t' = 0$ and the phase separation disappears for negative $t' = -0.2$. We think that there is a possibility that the phase separation will disappear as the wave function is optimized further by multiplying by operators P_G and $\exp(-\lambda'K)$.

7. Summary

We investigated the ground-state properties of the two-dimensional Hubbard model by using the optimization variational Monte Carlo method. We used the exponential type wave function given in the form $\exp(-\lambda S)$ with an appropriate operator S and a variational parameter λ . With our wave function, the ground-state energy is lowered greatly and the energy expectation value is lower than that obtained by any other wave function such as the Gutzwiller wave function and also several proposed wave functions with many variational parameters. The ground-state energy is lowered due to the kinetic-energy gain coming from $\exp(-\lambda K)$.

The antiferromagnetic state is very stable near half-filling (with no carriers) in the 2D Hubbard model the also the three-band d-p model. The AF correlation is suppressed as the doping rate of holes increases. As the strength of the on-site Coulomb interaction U changes, the crossover occurs between weakly correlated region and strongly correlated region. In the strongly correlated region, where U is larger than U_c which is of the order of the bandwidth, the AF correlation is suppressed. A decrease of AF correlation indicates an increase in spin and charge fluctuation. This fluctuation is caused by an increase in kinetic energy and would induce electron pairing. We expect that this would cause high-temperature superconductivity.

Lastly we supplement the crossover. We expect that the crossover behavior is a universal phenomenon. The s-d model shows a crossover from weakly coupling to strongly coupling regions as the temperature decreases [77–79]. The logarithmic dependence of the resistivity appears due to an anomaly associated with the crossover [80–85]. The two-impurity Kondo problem also shows a crossover [86–88]. There may be a universal class that includes the Kondo effect, QCD [89], BCS-BEC crossover [90], Superconductivity, sine-Gordon model [91–93]. Fluctuations associated with the crossover may be represented by excitation modes that occur near a phase transition [94].

Author Contributions: Conceptualization, T.Y. and M.M.; Methodology, T.Y. and K.Y.; Validation, T.Y., M.M. and K.Y.; Writing-Original Draft Preparation, T.Y.

Funding: This work was supported by a Grant-in-Aid for Scientific Research from the Ministry of Education, Culture, Sports, Science and Technology of Japan (Grant No. 17K05559).

Acknowledgments: A part of computations was supported by the Supercomputer Center of the Institute for Solid State Physics, the University of Tokyo.

Conflicts of Interest: The authors declare no conflict of interest.

Abbreviations

The following abbreviations are used in this manuscript:

VMC	variational Monte Carlo method
AF	antiferromagnetic
SC	superconductivity or superconducting
2D	two-dimensional
AFI	antiferromagnetic insulator
PI	paramagnetic insulator

References

1. Bednorz, J.B.; Müller, K.A. Possible high T_c superconductivity in the Ba-La-Cu-O system. *Z. Phys.* **1986**, *B64*, 189–193. [[CrossRef](#)]
2. Emery, V.J. Theory of high- T_c superconductivity in oxides. *Phys. Rev. Lett.* **1987**, *58*, 2794. [[CrossRef](#)] [[PubMed](#)]
3. Hirsch, J.E.; Loh, E.Y.; Scalapino, D.J.; Tang, S. Pairing interaction in CuO clusters. *Phys. Rev. B* **1989**, *B39*, 243. [[CrossRef](#)]
4. Scalettar, R.T.; Scalapino, D.J.; Sugar, R.L.; White, S.R. Antiferromagnetic, charge-transfer, and pairing correlations in the three-band Hubbard model. *Phys. Rev. B* **1991**, *B44*, 770. [[CrossRef](#)]
5. Oguri, A.; Asahatam, T.; Maekawa, S. Gutzwiller wave function in the three-band Hubbard model: A variational Monte Carlo study. *Phys. Rev. B* **1994**, *B49*, 6880. [[CrossRef](#)]
6. Koikegami, S.; Yamada, K. Antiferromagnetic and superconducting correlations on the d-p model. *J. Phys. Soc. Jpn.* **2000**, *69*, 768–776. [[CrossRef](#)]
7. Yanagisawa, T.; Koike, S.; Yamaji, K. Ground state of the three-band Hubbard model. *Phys. Rev. B* **2001**, *B64*, 184509. [[CrossRef](#)]
8. Koikegami, S.; Yanagisawa, T. Superconducting gap of the two-dimensional d-p model with small U_d . *J. Phys. Soc. Jpn.* **2001**, *70*, 3499–3502. [[CrossRef](#)]
9. Yanagisawa, T.; Koike, S.; Yamaji, K. Lattice distortions, incommensurability, and stripes in the electronic model for high- T_c cuprates. *Phys. Rev. B* **2003**, *B67*, 132408. [[CrossRef](#)]
10. Koikegami, S.; Yanagisawa, T. Superconductivity in Sr_2RuO_4 mediated by Coulomb scattering. *Phys. Rev. B* **2003**, *B67*, 134517. [[CrossRef](#)]
11. Koikegami, S.; Yanagisawa, T. Superconductivity in multilayer perovskite. *J. Phys. Soc. Jpn.* **2006**, *75*, 034715. [[CrossRef](#)]
12. Yanagisawa, T.; Miyazaki, M.; Yamaji, K. Incommensurate antiferromagnetism coexisting with superconductivity in two-dimensional d-p model. *J. Phys. Soc.* **2009**, *78*, 031706. [[CrossRef](#)]
13. Weber, C.; Lauchi, A.; Mila, F.; Giamarchi, T. Orbital currents in extended Hubbard model of High- T_c cuprate superconductors. *Phys. Rev. Lett.* **2009**, *102*, 017005. [[CrossRef](#)] [[PubMed](#)]
14. Lau, B.; Berciu, M.; Sawatzky, G.A. High spin polaron in lightly doped CuO_2 planes. *Phys. Rev. Lett.* **2011**, *106*, 036401. [[CrossRef](#)] [[PubMed](#)]
15. Weber, C.; Giamarchi, T.; Varma, C.M. Phase diagram of a three-orbital model for high- T_c cuprate superconductors. *Phys. Rev. Lett.* **2014**, *112*, 117001. [[CrossRef](#)] [[PubMed](#)]
16. Avella, A.; Mancini, F.; Paolo, F.; Plekhanov, E. Emery vs Hubbard model for cuprate superconductors: A composite operator method study. *Eur. Phys. J.* **2013**, *B86*, 265. [[CrossRef](#)]
17. Ebrahimnejad, H.; Sawatzky, G.A.; Berciu, M. Differences between the insulating limit quasiparticles of one-band and three-band cuprate models. *J. Phys. Cond. Matter* **2016**, *28*, 105603. [[CrossRef](#)] [[PubMed](#)]
18. Tamura, S.; Yokoyama, H. Variational study of magnetic ordered state in d-p model. *Phys. Procedia* **2016**, *81*, 5. [[CrossRef](#)]
19. Hubbard, J. Electron correlations in narrow energy bands. *Proc. Roy. Soc. Lond.* **1963**, *276*, 238–257. [[CrossRef](#)]
20. Hubbard, J. Electron correlations in narrow energy bands III. *Proc. Roy. Soc. Lond.* **1964**, *281*, 401–419. [[CrossRef](#)]
21. Gutzwiller, M.C. Effect of correlation on the ferromagnetism of transition metals. *Phys. Rev. Lett.* **1963**, *10*, 159. [[CrossRef](#)]

22. Zhang, S.; Carlson, J.; Gubernatis, J.E. Constrained path Monte Carlo method for fermion ground states. *Phys. Rev. B* **1997**, *B55*, 7464. [[CrossRef](#)]
23. Zhang, S.; Carlson, J.; Gubernatis, J.E. Pairing correlation in the two-dimensional Hubbard model. *Phys. Rev. Lett.* **1997**, *78*, 4486. [[CrossRef](#)]
24. Yanagisawa, T.; Shimoi, Y. Exact results in strongly correlated electrons. *Int. J. Mod. Phys.* **1996**, *B10*, 3383. [[CrossRef](#)]
25. Yanagisawa, T.; Shimoi, Y. Ground state of the Kondo-Hubbard model at half-filling. *Phys. Rev. Lett.* **1995**, *74*, 4939. [[CrossRef](#)] [[PubMed](#)]
26. Nakanishi, T.; Yamaji, K.; Yanagisawa, T. Variational Monte Carlo indications of d-wave superconductivity in the two-dimensional Hubbard model. *J. Phys. Soc. Jpn.* **1997**, *66*, 294–297. [[CrossRef](#)]
27. Yamaji, K.; Yanagisawa, T.; Nakanishi, T.; Koike, S. Variational Monte Carlo study on the superconductivity in the two-dimensional Hubbard model. *Physica* **1998**, *C304*, 225–238. [[CrossRef](#)]
28. Yamaji, K.; Yanagisawa, T.; Koike, S. Bulk limit of superconducting condensation energy in 2D Hubbard model. *Physica* **2000**, *284*, 415–416. [[CrossRef](#)]
29. Yamaji, K.; Yanagisawa, T.; Miyazaki, M.; Kadono, R. Superconducting condensation energy of the two-dimensional Hubbard model in the large-negative- t' region. *J. Phys. Soc. Jpn.* **2011**, *80*, 083702. [[CrossRef](#)]
30. Hardy, T.M.; Hague, P.; Samson, J.H.; Alexandrov, A.S. Superconductivity in a Hubbard-Fröhlich model in cuprates. *Phys. Rev. B* **2009**, *B79*, 212501. [[CrossRef](#)]
31. Yanagisawa, T.; Miyazaki, M.; Yamaji, K. Correlated-electron systems and high-temperature superconductivity. *J. Mod. Phys.* **2013**, *4*, 33. [[CrossRef](#)]
32. Bulut, N. $d_{x^2-y^2}$ superconductivity and the Hubbard model. *Adv. Phys.* **2002**, *51*, 1587–1667. [[CrossRef](#)]
33. Yokoyama, H.; Tanaka, Y.; Ogata, M.; Tsuchiura, H. Crossover of superconducting properties and kinetic-energy gain in two-dimensional Hubbard model. *J. Phys. Soc. Jpn.* **2004**, *73*, 1119–1122. [[CrossRef](#)]
34. Aimi, T.; Imada, M. Does simple two-dimensional Hubbard model account for high- T_c superconductivity in copper oxides? *J. Phys. Soc. Jpn.* **2007**, *76*, 113708. [[CrossRef](#)]
35. Miyazaki, M.; Yanagisawa, T.; Yamaji, K. Diagonal stripe states in the eight-doping region in the two-dimensional Hubbard model. *J. Phys. Soc. Jpn.* **2004**, *73*, 1643–1646. [[CrossRef](#)]
36. Yanagisawa, T. Phase diagram of the t - U^2 Hamiltonian of the weak coupling Hubbard model. *N. J. Phys.* **2008**, *10*, 023014. [[CrossRef](#)]
37. Yanagisawa, T. Enhanced pair correlation functions in the two-dimensional Hubbard model. *N. J. Phys.* **2013**, *15*, 033012. [[CrossRef](#)]
38. Yanagisawa, T. Crossover from weakly to strongly correlated regions in the two-dimensional Hubbard model—Off-diagonal Monte Carlo studies of Hubbard model II. *J. Phys. Soc. Jpn.* **2016**, *85*, 114707. [[CrossRef](#)]
39. Noack, R.M.; White, S.R.; Scalapino, D.J. The doped two-chain Hubbard model. *Europhys. Lett.* **1995**, *30*, 163. [[CrossRef](#)]
40. Noack, R.M.; Bulut, N.; Scalapino, D.J.; Zacher, M.J. Enhanced $d_{x^2-y^2}$ pairing correlations in the two-leg Hubbard ladder. *Phys. Rev. B* **1997**, *B56*, 7162. [[CrossRef](#)]
41. Yamaji, K.; Shimoi, Y.; Yanagisawa, T. Superconductivity indications of the two-chain Hubbard model due to the two-band effect. *Physica* **1994**, *C235*, 2221–2222. [[CrossRef](#)]
42. Yanagisawa, T.; Shimoi, Y.; Yamaji, K. Superconducting phase of a two-chain Hubbard model. *Phys. Rev. B* **1995**, *B52*, R3860. [[CrossRef](#)]
43. Nakano, T.; Kuroki, K.; Onari, S. Superconductivity due to spin fluctuations originating from multiple Fermi surfaces in the double chain superconductor $\text{Pr}_2\text{Ba}_4\text{Cu}_7\text{O}_{15-\delta}$. *Phys. Rev. B* **2007**, *B76*, 014515. [[CrossRef](#)]
44. Mott, N. F. *Metal-Insulator Transitions*; Taylor and Francis Ltd.: London, UK, 1974.
45. Moriya, T. *Spin Fluctuations in Itinerant Electron Magnetism*; Springer-Verlag: Berlin, Germany, 1985.
46. Yosida, K. *Theory of Magnetism*; Springer-Verlag: Berlin, Germany, 1996.
47. Tranquada, J.M.; Axe, J.D.; Ichikawa, N.; Nakamura, Y.; Uchida, S.; Nachumi, B. Neutron-scattering study of stripe-phase order of holes and spins in $\text{La}_{1.48}\text{Nd}_{0.4}\text{Sr}_{0.12}\text{CuO}_4$. *Phys. Rev. B* **1996**, *B54*, 7489. [[CrossRef](#)]
48. Suzuki, T.; Goto, T.; Chiba, K.; Shinoda, T.; Fukase, T.; Kimura, H.; Yamada, K.; Ohashi, M.; Yamaguchi, Y. Observation of modulated magnetic long-range order in $\text{La}_{1.88}\text{Sr}_{0.12}\text{CuO}_4$. *Phys. Rev. B* **1998**, *B57*, R3229. [[CrossRef](#)]

49. Yamada, K.; Lee, C.H.; Kurahashi, K.; Wada, J.; Wakimoto, S.; Ueki, S.; Kimura, H.; Endoh, Y.; Hosoya, S.; Shirane, G.; et al. Doping dependence of the spatially modulated dynamical spin correlations and the superconducting-transition temperature in $\text{La}_{2-x}\text{Sr}_x\text{CuO}_4$. *Phys. Rev. B* **1998**, *B57*, 6165. [[CrossRef](#)]
50. Arai, M.; Nishijima, T.; Endoh, Y.; Egami, T.; Tajima, S.; Tomimoto, K.; Shiohara, Y.; Takahashi, M.; Garrett, A.; Bennington, S.M. Incommensurate spin dynamics of underdoped superconductor $\text{YBa}_2\text{Cu}_3\text{Y}_{6.7}$. *Phys. Rev. Lett.* **1999**, *83*, 608. [[CrossRef](#)]
51. Mook, H.A.; Dai, P.; Dogan, F.; Hunt, R.D. One-dimensional nature of the magnetic fluctuations in $\text{YBa}_2\text{Cu}_3\text{O}_{6.6}$. *Nature* **2000**, *404*, 729. [[CrossRef](#)] [[PubMed](#)]
52. Wakimoto, S.; Birgeneau, R.J.; Kastner, M.A.; Lee, Y.S.; Erwin, R.; Gehring, P.M.; Lee, S.H.; Fujita, M.; Yamada, K.; Endoh, Y.; et al. Direct observation of a one-dimensional static spin modulation in insulating $\text{La}_{1.95}\text{Sr}_{0.05}\text{CuO}_4$. *Phys. Rev. B* **2000**, *B61*, 3699. [[CrossRef](#)]
53. Bianconi, A.; Saini, N.L.; Lanzara, A.; Missori, M.; Rossetti, T.; Oyanagi, H.; Yamaguchi, H.; Oka, K.; Ito, T. Determination of the local lattice distortions in the CuO_2 plane of $\text{La}_{1.85}\text{Sr}_{0.15}\text{CuO}_4$. *Phys. Rev. Lett.* **1996**, *76*, 3412. [[CrossRef](#)] [[PubMed](#)]
54. Bianconi, A. Quantum materials: shape resonances in superstripes. *Nat. Phys.* **2013**, *9*, 536. [[CrossRef](#)]
55. Hoffman, J.E.; McElroy, K.; Lee, D.H.; Lang, K.M.; Eisaki, H.; Uchida, S.; Davis, J.C. Imaging quasiparticle interference in $\text{Bi}_2\text{Sr}_2\text{CaCu}_2\text{O}_{8+\delta}$. *Science* **2002**, *295*, 466. [[CrossRef](#)] [[PubMed](#)]
56. Wise, W.D.; Boyer, M.C.; Chatterjee, K.; Kondo, T.; Takeuchi, T.; Ikuta, H.; Wang, Y.; Hudson, E.W. Charge-density-wave origin of cuprate checkerboard visualized by scanning tunnelling microscopy. *Nat. Phys.* **2008**, *4*, 696. [[CrossRef](#)]
57. Hanaguri, T.; Lupien, C.; Kohsaka, Y.; Lee, D.H.; Azuma, M.; Takano, M.; Takagi, H.; Davis, J.C. A checkerboard electronic crystal state in lightly hole-doped $\text{Ca}_{2-x}\text{Na}_x\text{CuO}_2\text{Cl}_2$. *Nature* **2004**, *430*, 1001. [[CrossRef](#)] [[PubMed](#)]
58. Miyazaki, M.; Yanagisawa, T.; Yamaji, K. Checkerboard states in the two-dimensional Hubbard model with the Bi2212-type band. *J. Phys. Soc. Jpn.* **2009**, *78*, 043706. [[CrossRef](#)]
59. Koike, S.; Yamaji, K.; Yanagisawa, T. Effect of the medium-range transfer energies to the superconductivity in the two-chain Hubbard model. *J. Phys. Soc. Jpn.* **1999**, *68*, 1657–1663. [[CrossRef](#)]
60. Yanagisawa, T.; Koike, S.; Yamaji, K. Off-diagonal wave function Monte Carlo Studies of Hubbard model I. *J. Phys. Soc. Jpn.* **1998**, *67*, 3867–3874. [[CrossRef](#)]
61. Yanagisawa, T.; Miyazaki, M. Mott transition in cuprate high-temperature superconductors. *Eur. Phys. Lett.* **2014**, *107*, 27004. [[CrossRef](#)]
62. Yanagisawa, T.; Miyazaki, M.; Yamaji, K. Optimized wave function by kinetic renormalization effect in strongly correlated region of the three-band Hubbard model. *J. Phys. Conf. Ser.* **2018**, *1054*, 012017. [[CrossRef](#)]
63. McElroy, K.; Simmonds, R.W.; Hoffman, J.E.; Lee, D.H.; Orenstein, J.; Eisaki, H.; Uchida, S.; Davis, J.C. Relating atomic-scale electronic phenomena to wave-like quasiparticle states in superconducting $\text{Bi}_2\text{Sr}_2\text{CaCu}_2\text{O}_{8+\delta}$. *Nature* **2003**, *422*, 592. [[CrossRef](#)] [[PubMed](#)]
64. Hussey, N.E.; Abdel-Jawad, M.; Carrington, A.; Mackenzie, A.P.; Balicas, L. A coherent three-dimensional Fermi surface in a high-transition-temperature superconductor. *Nature* **2003**, *425*, 814. [[CrossRef](#)] [[PubMed](#)]
65. Weber, C.; Haule, K.; Kotliar, G. Critical weights and waterfalls in doped charge-transfer insulators. *Phys. Rev. B* **2008**, *B78*, 134519. [[CrossRef](#)]
66. Hybertsen, M. S.; Schlüter, M.; Christensen, N.E. Calculation of Coulomb-interaction parameter for La_2CuO_4 using a constrained-density-functional approach. *Phys. Rev. B* **1989**, *B39*, 9028. [[CrossRef](#)]
67. Eskes, H.; Sawatzky, G.A.; Feiner, L.F. Effective transfer for singlets formed by hole doping in the high- T_c superconductors. *Physica* **1989**, *C160*, 424–430. [[CrossRef](#)]
68. McMahan, A.K.; Annett, J.F.; Martin, R.M. Cuprate parameters from numerical Wannier functions. *Phys. Rev. B* **1990**, *B42*, 6268. [[CrossRef](#)]
69. Eskes, H.; Sawatzky, G. Single-, triple-, or multiple-band Hubbard models. *Phys. Rev. B* **1991**, *B43*, 119. [[CrossRef](#)]
70. Otsuka, H. Variational Monte Carlo studies of the Hubbard model in one- and two-dimensions. *J. Phys. Soc. Jpn.* **1992**, *61*, 1645–1656. [[CrossRef](#)]
71. Yanagisawa, T.; Koike, S.; Yamaji, K. d -wave state with multiplicative correlation factors for the Hubbard model. *J. Phys. Soc. Jpn.* **1999**, *68*, 3608–3614. [[CrossRef](#)]

72. Eichenberger, D.; Baeriswyl, D. Superconductivity and antiferromagnetism in the-dimensional Hubbard model: A variational study. *Phys. Rev. B* **2007**, *B76*, 180504. [[CrossRef](#)]
73. Baeriswyl, D.; Eichenberger, D.; Menteshashvili, M. Variational ground states of the two-dimensional Hubbard model. *N. J. Phys.* **2009**, *11*, 075010. [[CrossRef](#)]
74. Baeriswyl, D. Superconductivity in the repulsive Hubbards model. *J. Supercond. Novel Magn.* **2011**, *24*, 1157–1159. [[CrossRef](#)]
75. Yanagisawa, T. Quantum Monte Carlo diagonalization for many-fermion systems. *Phys. Rev. B* **2007**, *B75*, 224503. [[CrossRef](#)]
76. Misawa, T.; Imada, M. Origin of high- T_c superconductivity in doped Hubbard models and their extensions: Roles of uniform charge fluctuations. *Phys. Rev. B* **2014**, *B90*, 115137. [[CrossRef](#)]
77. Kondo, J. *The Physics of Dilute Magnetic Alloys*; Cambridge University Press: Cambridge, UK, 2012.
78. Yuval, G.; Anderson, P.W. Exact results for the Kondo problem: one-body theory and extension to finite temperature. *Phys. Rev. B* **1970**, *B1*, 1522. [[CrossRef](#)]
79. Wilson, K.G. The renormalization group: Critical phenomena and the Kondo problem. *Rev. Mod. Phys.* **1975**, *47*, 773. [[CrossRef](#)]
80. Nagaoka, Y. Self-consistent treatment of Kondo's effect in dilute alloys. *Phys. Rev. B* **1965**, *138*, A1112. [[CrossRef](#)]
81. Zittartz, J.; Müller-Hartmann, E. Green's function theory of the Kondo effect in dilute magnetic alloys. *Z. Phys.* **1968**, *212*, 380–407. [[CrossRef](#)]
82. Anderson, P.W.; Yuval, G.; Hamann, D.R. Exact results in the Kondo problem II. Scaling theory, qualitatively correct solution, and some new results on one-dimensional classical statistical models. *Phys. Rev. B* **1970**, *B1*, 4464. [[CrossRef](#)]
83. Yanagisawa, T. Kondo effect in the presence of spin-orbit coupling. *J. Phys. Soc. Jpn.* **2012**, *81*, 094713. [[CrossRef](#)]
84. Yanagisawa, T. Kondo effect in Dirac systems. *J. Phys. Soc. Jpn.* **2015**, *84*, 074705. [[CrossRef](#)]
85. Yanagisawa, T. Dirac fermions and Kondo effect. *J. Phys. Conf. Ser.* **2015**, *603*, 012014. [[CrossRef](#)]
86. Jayaprakash, C.; Krishna-murthy, H.R.; Wilkins, J.W. Two-impurity Kondo problem. *Phys. Rev. Lett.* **1981**, *47*, 737. [[CrossRef](#)]
87. Jones, B.A.; Varma, C.M. Critical point in the solution of the two-impurity Kondo problem. *Phys. Rev. B* **1989**, *B40*, 324. [[CrossRef](#)]
88. Yanagisawa, T. Ground state and staggered susceptibility of the two-impurity Kondo problem. *J. Phys. Soc. Jpn.* **1989**, *60*, 29–32. [[CrossRef](#)]
89. Ellis, R.K.; Stirling, W.J.; Webber, B.R. *QCD and Collider Physics*; Cambridge University Press: Cambridge, UK, 1996.
90. Nozieres, P.; Schmitt-Rink, S. Bose condensation in an attractive fermi gas: From weak to strong coupling superconductivity. *J. Low Temp. Phys.* **1985**, *59*, 195–211. [[CrossRef](#)]
91. Rajaraman, R. *Solitons and Instantons*; North-Holland: Amsterdam, The Netherlands, 1989.
92. Solyom, J. The Fermi gas model of one-dimensional conductors. *Adv. Phys.* **1979**, *28*, 201–303. [[CrossRef](#)]
93. Yanagisawa, T. Chiral sine-Gordon model. *Eur. Lett.* **2016**, *113*, 41001. [[CrossRef](#)]
94. Yanagisawa, T. Nambu-Goldstone bosons characterized by the order parameters in spontaneous symmetry breaking. *J. Phys. Soc. Jpn.* **2017**, *86*, 104711. [[CrossRef](#)]

